Electron-Donating Alkoxy-Group-Driven Synthesis of Heteroleptic Tris(phthalocyaninato) Lanthanide(III) Triple-Deckers with Symmetrical Molecular Structure

Peihua Zhu,[a] Na Pan,[a] Renjie Li,[a] Jianmin Dou,[b] Ying Zhang,[a] Diana Y. Y. Cheng,[c] Daqi Wang,[b] Dennis K. P. Ng,[c] and Jianzhuang Jiang*[a]

Abstract: Reaction of heteroleptic bis(phthalocyaninato) lanthanide compounds [(Pc)M{Pc(OC_8H_{17})$_8$}] [H_2Pc = unsubstituted phthalocyanine; $H_2Pc(OC_8H_{17})_8$ = 2,3,9,10,16,17,23,24-octakis(octyloxy)phthalocyanine] with monomeric complexes [(Pc)M(acac)] (Hacac = acetylacetone), both of which generated in situ, led to the isolation of heteroleptic phthalocyaninato-[2,3,9,10,16,17,23,24-octakis(octyloxy)-phthalocyaninato] lanthainde(III) triple-decker complexes [(Pc)M{Pc(OC_8H_{17})$_8$}] (M = Gd–Lu) (**1**–**8**) as the sole product. Heterodinuclear analogues [(Pc)Lu{Pc(OC_8H_{17})$_8$}M(Pc)] (M = Gd–Yb) (**9**–**15**) were obtained in a similar manner from the reaction of [(Pc)M{Pc(OC_8H_{17})$_8$}] (M = Gd–Yb) and [(Pc)Lu(acac)]. The molecular structures of the herterodinuclear compound [(Pc)Lu{Pc(OC_8H_{17})$_8$}Er(Pc)] (**13**) and its homodinuclear counterparts [(Pc)M{Pc(OC_8H_{17})$_8$}M(Pc)] (M = Er, Lu) (**5**, **8**) have been determined by X-ray diffraction analysis; these structures exhibit a symmetrical molecular structure with one inner planar Pc(OC_8H_{17})$_8$ ligand and two outer domed Pc ligands. In addition to various spectroscopic analyses, the electrochemistry of these compounds has also been studied by cyclic voltammetry (CV) and differential pulse voltammetry (DPV) methods, revealing the gradually enhanced π–π interactions among the phthalocyanine rings in the triple-deckers along with the lanthanide contraction.

Keywords: lanthanides · phthalocyanines · sandwich complexes · triple-decker complexes

Introduction

Triple-decker tris(phthalocyaninato) rare-earth-metal complexes were initially studied as a result of the research on their bis(phthalocyaninato) derivatives for the purpose of further investigation into the interaction between the phthalocyanine rings in the "stacked π-conjugated molecules".[1–6] Very recently, they have started to attract interest as they are good systems to study for the interaction between two 4f-electonic ions in an isolated environment,[7–9] in addition to the benzimidazole, pyridine, and dipicolinic acid rare-earth-metal complexes with triple-helix structures.[10–14]

The first tris(phthalocyaninato) rare-earth-metal compound was homoleptic [$Y_2(Pc)_3$] reported in 1986 by Takahashi and Kasuga as a side-product in the synthesis of double-decker [$Y(Pc)_2$].[1] Later, homoleptic-substituted tris(phthalocyaninato) rare-earth-metal analogues [$M_2\{Pc(OC_4H_9)_8\}_3$] [M = La, Dy, Yb, Lu; $H_2Pc(OC_4H_9)_8$ = 2,3,9,10,16,17,23,24-octakis(butyloxy)phthalocyanine], derived from metal-free phthalocyanine ligands and rare-earth-metal acetates, were also reported by this group.[2] Quite recently, L'Her detailed the synthesis, characterization, and electrochemical behavior of the tris(1,2-naphthalocyaninato) lutetium compound [Lu_2(1,2-Nc)$_3$] (H_2(1,2-Nc) = 1,2-naphthalocyanine).[3] Ishikawa and co-workers prepared the first heteroleptic phthalocyaninato triple-decker complex [(Pc)Lu{Pc(15C5)$_4$}Lu(Pc)] (H_2Pc(15C5)$_4$ = tetra-([15]crown-5)-substituted phthalocyanine) and studied its

---

[a] P. Zhu, N. Pan, R. Li, Y. Zhang, Prof. J. Jiang
Department of Chemistry, Shandong University
Jinan 250100 (China)
Fax: (+86) 531-856-5211
E-mail: jzjiang@sdu.edu.cn

[b] Prof. J. Dou, Prof. D. Wang
Department of Chemistry, Liaocheng University
Liaocheng 252000 (China)

[c] D. Y. Y. Cheng, Prof. D. K. P. Ng
Department of Chemistry
The Chinese University of Hong Kong
Shatin, N.T., Hong Kong (China)

Supporting information for this article is available on the WWW under http://www.chemeurj.org/ or from the author.

DOI: 10.1002/chem.200400879

electronic absorption and MCD spectra.[4] As part of the efforts to developing novel species of sandwich tetrapyrrole rare-earth-metal complexes, we have described the synthesis of a series of heteroleptic phthalocyaninato rare-earth-metal triple-decker complexes [(Pc)M{Pc(OC_8H_{17})$_8$}M{Pc(OC_8H_{17})$_8$}] (M = Nd, Sm, Eu, Gd, Tb, Dy, Ho, Er, Tm, Y) and studied their ^{1}H NMR spectroscopic and electrochemical properties.[5,6] We also isolated tris(phthalocyaninato) rare-earth-metal triple-deckers [(Pc)M{Pc(OC_8H_{17})$_8$}M(Pc)] in very low yield as the side-product of the reaction among M(acac)$_3$·nH$_2$O, Li$_2$(Pc), and [M{Pc(OC_8H_{17})$_8$}$_2$].[5,6] By employing a similar procedure, Ishikawa and co-workers prepared the series of rare-earth-metal analogues [(Pc)M(Pc)M′{Pc(OC_4H_9)$_8$}] (M = or ≠M′ = Tb–Yb, Y) and investigated the interaction between the two rare-earth-metal ions by means magnetic and NMR measurements.[7–9]

In the present paper, we report the electron-donating octyloxy-group-driven synthesis and molecular structure of the series of heteroleptic tris(phthalocyaninato) complexes of both homo- and heterodinuclear lanthanide metals [(Pc)M{Pc(OC_8H_{17})$_8$}M(Pc)] (M = Gd–Lu) (**1**–**8**) and [(Pc)Lu{Pc(OC_8H_{17})$_8$}M(Pc)] (M = Gd–Yb) (**9**–**15**). Their spectroscopic and electrochemical properties have also been comparatively studied to reveal the nature of π–π interactions in the triple-decker molecules.

Results and Discussion

Synthesis: The history of the tris(phthalocyaninato) rare-earth-metal complexes is relatively short compared with that of bis(phthalocyaninato) rare-earth-metal counterparts.[15,16] The heteroleptic tris(phthalocyaninato) rare-earth-metal compounds in which two different phthalocyanine ligands are contained in one molecule are still scare and are limited to [(Pc)Lu{Pc(15C5)$_4$}Lu(Pc)],[4] [(Pc)M{Pc(OC_8H_{17})$_8$}M{Pc(OC_8H_{17})$_8$}] (M = Nd, Sm, Eu, Gd, Tb, Dy, Ho, Er, Tm, Y),[5,6] and [(Pc)M(Pc)M′{Pc(OC_4H_9)$_8$}] (M = or ≠M′ = Tb-Yb, Y)[7–9] reported very recently by either Ishikawa or Jiang and co-workers. Except for [(Pc)Lu{Pc(15C5)$_4$}Lu(Pc)], which was isolated by using monomeric complex [Lu(Pc)(OAc)] and metal-free H$_2$[Pc(15C5)$_4$] as starting materials, all the remaining heteroleptic tris(phthalocyaninato) rare-earth-metal(III) triple-decker complexes were prepared by condensation of monomeric [(Pc′)M(X)] (Pc′ = Pc, Pc(OC_4H_9)$_8$; X = acac, OAc) generated in situ and [M(Pc′)$_2$] (Pc′ = Pc(OC_8H_{17})$_8$, Pc) in refluxing n-octanol or 1,2,4-trichlorobenzene (TCB). Under the experimental conditions given in reference [5], the isolation, albeit in low yield, of unexpected heteroleptic triple-deckers with the symmetrical structure [(Pc)M{Pc(OC_8H_{17})$_8$}M(Pc)] is considered to result from the reaction of excess [(Pc)M(acac)] with the scrambled heteroleptic intermediate [(Pc)M{Pc(OC_8H_{17})$_8$}], which results from the thermolysis of [(Pc)M{Pc(OC_8H_{17})$_8$}M{Pc(OC_8H_{17})$_8$}] at high temperature. This postulate is clearly verified by the results of the present investigations; the condensation between [(Pc)M(acac)] and [(Pc)M{Pc(OC_8H_{17})$_8$}] lead to the isolation of [(Pc)M{Pc(OC_8H_{17})$_8$}M(Pc)] (M = Gd–Lu) (**1**–**8**) as the sole product. Further proof comes from the generation of heterodinuclear lanthanide complexes [(Pc)Lu{Pc(OC_8H_{17})$_8$}M(Pc)] (M = Gd-Yb) (**9**–**15**) through the reaction of [(Pc)Lu(acac)] and [(Pc)M{Pc(OC_8H_{17})$_8$}] (M = Gd-Yb). It is worth noting that triple-deckers with symmetrical structure were isolated as the sole products without detection of the other possible triple-decker species, for example, [(Pc)M(Pc)M{Pc(OC_8H_{17})$_8$}] under the present experimental conditions. This suggests that the electronic effect in the heteroleptic double-decker molecule of [(Pc)M{Pc(OC_8H_{17})$_8$}] dominates in the

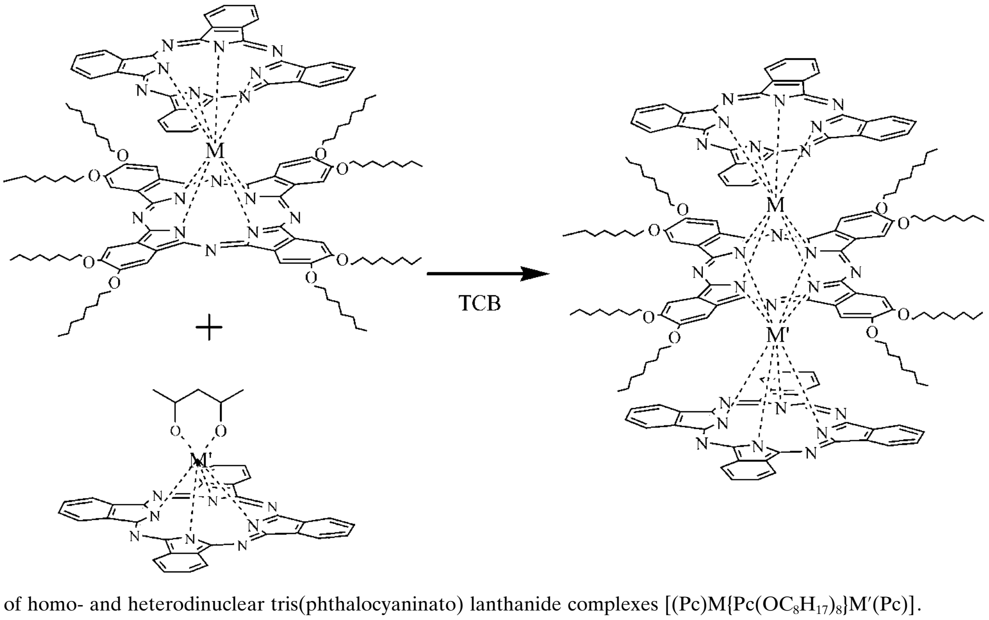

Scheme 1. Synthesis of homo- and heterodinuclear tris(phthalocyaninato) lanthanide complexes [(Pc)M{Pc(OC_8H_{17})$_8$}M′(Pc)].

product formed the reaction between [(Pc)M(acac)] and [(Pc)M{Pc(OC_8H_{17})$_8$}] and drives the formation of triple-decker in the form of [(Pc)M{Pc(OC_8H_{17})$_8$}M(Pc)] instead of [(Pc)M(Pc)M{Pc(OC_8H_{17})$_8$}], Scheme 1. The introduction of eight electron-donating octyloxy groups onto the peripheral positions of one phthalocyanine ring of the heteroleptic [(Pc)M{Pc(OC_8H_{17})$_8$}] makes its isoindole nitrogen atoms more electron-rich relative to those in the unsubstituted Pc ligand, and thus they coordinate more easily to the lanthanide ion of [(Pc)M(acac)] despite the possible steric hinderance, also due to the eight octyloxy side chains in the same Pc(OC_8H_{17})$_8$ ring.

Satisfactory elemental analysis results have been obtained for all these newly prepared hetero- and homodinuclear lanthanide triple-decker complexes **1**–**8** and **9**–**15**, which have good solubility in common organic solvents such as $CHCl_3$, CH_2Cl_2, and toluene, after repeated column chromatography and recrystallization, Table 1. They have also been characterized by MALDI-TOF mass spectrometry (Table 1) and ^{1}H NMR spectroscopy. Their sandwich triple-decker nature was further evidenced by single-crystal X-ray analysis for the homodinuclear complexes **5** and **8** and the heterodinuclear complex **13**.

Table 1. Analytical and mass spectrometric data for the heteroleptic triple-deckers **1**–**15**.[a]

Compound	m/z $[M]^+$/$[M+H]^+$[b]	Analysis [%] C	H	N
[(Pc)Gd{Pc(OC_8H_{17})$_8$}Gd(Pc)] (**1**)	2877.8 (2877.3)	66.39 (66.77)	6.09 (6.16)	11.53(11.68)
[(Pc)Tb{Pc(OC_8H_{17})$_8$}Tb(Pc)] (**2**)	2881.2 (2881.3)[c]	65.25 (66.70)	6.07 (6.16)	11.48 (11.67)
[(Pc)Dy{Pc(OC_8H_{17})$_8$}Dy(Pc)] (**3**)	2889.7 (2889.3)[c]	66.22 (66.53)	6.00 (6.14)	11.76 (11.64)
[(Pc)Ho{Pc(OC_8H_{17})$_8$}Ho(Pc)] (**4**)	2894.3 (2893.3)[c]	65.95 (66.42)	6.04 (6.13)	11.45 (11.62)
[(Pc)Er{Pc(OC_8H_{17})$_8$}Er(Pc)] (**5**)	2897.9 (2898.3)[c]	65.73 (66.31)	6.01 (6.12)	11.28 (11.60)
[(Pc)Tm{Pc(OC_8H_{17})$_8$}Tm(Pc)] (**6**)	2901.6 (2901.3)[c]	65.03 (66.24)	6.16 (6.12)	10.95 (11.59)
[(Pc)Yb{Pc(OC_8H_{17})$_8$}Yb(Pc)] (**7**)	2909.8 (2909.3)	66.00 (66.05)	6.09 (6.10)	11.65 (11.56)
[(Pc)Lu{Pc(OC_8H_{17})$_8$}Lu(Pc)] (**8**)	2913.8 (1913.3)	65.80 (65.96)	5.92 (6.09)	11.44 (11.54)
[(Pc)Lu{Pc(OC_8H_{17})$_8$}Gd(Pc)] (**9**)	2895.6 (2895.3)	66.18 (66.37)	6.44 (6.13)	10.80 (11.61)
[(Pc)Lu{Pc(OC_8H_{17})$_8$}Tb(Pc)] (**10**)	2897.2 (2897.3)	65.55 (66.33)	5.96 (6.12)	11.59 (11.61)
[(Pc)Lu{Pc(OC_8H_{17})$_8$}Dy(Pc)] (**11**)	2900.0 (2900.3)	66.12 (66.25)	5.96 (6.12)	11.78 (11.59)
[(Pc)Lu{Pc(OC_8H_{17})$_8$}Ho(Pc)] (**12**)	2903.3 (2903.3)	66.05 (66.19)	6.13 (6.11)	11.34 (11.58)
[(Pc)Lu{Pc(OC_8H_{17})$_8$}Er(Pc)] (**13**)	2905.6 (2905.3)	66.44 (66.14)	6.43 (6.11)	10.87 (11.57)
[(Pc)Lu{Pc(OC_8H_{17})$_8$}Tm(Pc)] (**14**)	2907.6 (2907.3)	66.01 (66.10)	6.19 (6.10)	11.09 (11.57)
[(Pc)Lu{Pc(OC_8H_{17})$_8$}Yb(Pc)] (**15**)	2911.6 (2911.3)	65.52 (66.01)	6.03 (6.09)	11.27 (11.55)

[a] Calculated values given in parentheses. [b] By MALDI-TOF mass spectrometry. [c] Cited from reference [5a].

Table 2. Electronic absorption data for the triple-deckers **1**–**15** in $CHCl_3$.

	λ_{max} [nm^{-1}] ($\log \varepsilon$)			
1	295 (4.93)	333 (5.09)	643 (5.25)	692 (4.55)
2	294 (4.93)	333 (5.08)	642 (5.23)	698 (4.51)
3	295 (4.96)	333 (5.14)	640 (5.13)	703 (4.60)
4	295 (4.92)	331 (5.11)	639 (5.18)	707 (4.56)
5	295 (4.93)	331 (5.12)	638 (5.22)	711 (4.58)
6	296 (4.88)	332 (5.08)	637 (5.23)	714 (4.54)
7	296 (4.81)	332 (5.00)	634 (5.12)	720 (4.45)
8	296 (4.87)	331 (5.05)	634 (5.20)	722 (4.51)
9	295 (4.97)	331 (5.18)	641 (5.18)	706 (4.58)
10	295 (4.93)	332 (5.14)	640 (5.27)	708 (4.56)
11	295 (4.88)	332 (5.08)	638 (5.23)	711 (4.51)
12	296 (4.97)	333 (5.17)	635 (5.28)	713 (4.61)
13	296 (4.94)	332 (5.14)	635 (5.26)	716 (4.58)
14	296 (4.88)	332 (5.08)	634 (5.22)	718 (4.53)
15	296 (4.93)	332 (5.12)	632 (5.18)	719 (4.57)

The MALDI-TOF mass spectra of these compounds clearly showed intense signals for the molecular ion $[M]^+$. The isotopic pattern closely resembled that of the simulation as exemplified by the spectrum of the heterodinuclear analogue **11** given in Figure S1 (see the Supporting Information).

Electronic absorption spectra: The electronic absorption spectra of triple-decker complexes (**1**–**15**) were recorded in $CHCl_3$ and the data are summarized in Table 2. Figure 1 displays a typical UV-visible spectrum of heterodinuclear [(Pc)Lu{Pc(OC_8H_{17})$_8$}Tb(Pc)] (**10**) and those of its homodinuclear counterparts [(Pc)Tb{Pc(OC_8H_{17})$_8$}Tb(Pc)] (**2**) and [(Pc)Lu{Pc(OC_8H_{17})$_8$}Lu(Pc)] (**8**). They are analogous to those reported for related homo- and heteroleptic tris(phthalocyaninato) lanthanide compounds.[2,4] The absorption around 332 nm with a shoulder at higher energy (295 nm) can be attributed to the phthalocyaninato Soret bands for **1**–**15**. For the homodinuclear species **1**–**8**, the phthalocyaninato Q-bands appear around 634–643 nm as a very strong absorption with a weak satellite around 692–722 nm. It is clear that along with the decrease of the ionic size of the lanthanide from Gd to Lu, the Soret band for all the triple-deckers remains at almost the same position. However, the main Q-band with stronger intensity is blue-shifted and the satellite Q-band red-shifted for the series **1**–**8**. As a result, the splitting of the two Q-bands for the series of compounds **1**–**8** increases along with the lanthanide contraction (Figure 2), indicating the increasing π–π interaction among phthalocyanine ligands in the same order.

As shown in Table 2 and Figure 1, the electronic absorption spectra of heterodinuclear compounds **9**–**15** take the same features with those of homodinuclear analogues. Although the Soret band position remained almost unchanged, both the main and side Q-bands are shifted to the red or blue relative to those of homodinuclear counterparts, lying in the middle of the corresponding bands of the two homodinuclear counterparts. This suggests that the Q-band absorptions of heteroleptic phthalocyaninato compounds contain contributions from both unsubstituted and substituted

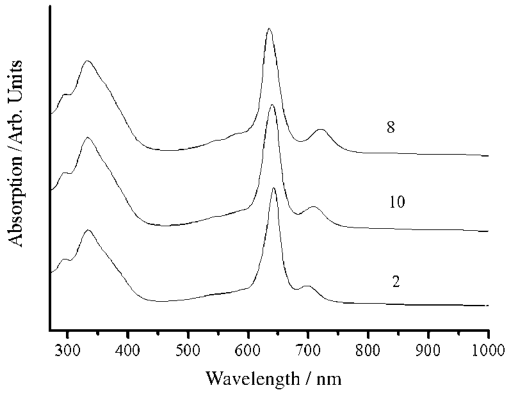

Figure 1. The electronic absorption spectra of [(Pc)Tb{Pc(OC_8H_{17})$_8$}-Tb(Pc)] (**2**), [(Pc)Lu{Pc(OC_8H_{17})$_8$}Tb(Pc)] (**10**) and [(Pc)Lu{Pc-(OC_8H_{17})$_8$}Lu(Pc)] (**8**) in $CHCl_3$.

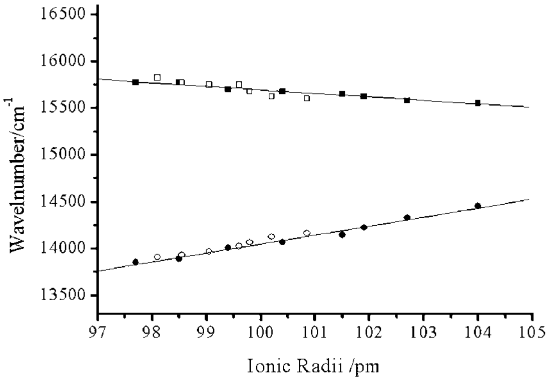

Figure 2. Plot of wavenumbers of the two Q-bands of [(Pc)M{Pc(OC_8H_{17})$_8$}M(Pc)] (**1**–**8**) (solid symbols) and [(Pc)Lu{Pc-(OC_8H_{17})$_8$}M(Pc)] (**9**–**15**) (open symbols) as a function of the ionic radius M^{III} and the mean ionic radius of Lu^{III} and M^{III}, respectively.

phthalocyanine ligands, due to the strong π–π interaction among phthalocyanine rings connected by two lanthanide ions. Nevertheless, the energies of the two Q-bands of these heterodinuclear lanthanide triple-decker complexes **9**–**15** fit the linear correlation established between the energies of the two Q-bands and ionic radii for homodinuclear lanthanide complexes **1**–**8** if the mean ionic radius of Lu and M is employed (Figure 2), also revealing the increasing π–π interaction among phthalocyanine ligands along with the lanthanide contraction.

NMR spectra: The ^{1}H NMR spectra of all the newly prepared triple-decker compounds except for [(Pc)Gd{Pc-(OC_8H_{17})$_8$}Gd(Pc)] (**1**) and [(Pc)Lu{Pc(OC_8H_{17})$_8$}Gd(Pc)] (**9**) have been recorded in $CDCl_3$ at room temperature. The assignment of the spectra for the homodinuclear complexes **7** and **8** is straightforward because of the resolved multiplicity in the signals for the alkyl-chain protons and the availability of [(Pc)Y{Pc(OC_8H_{17})$_8$}Y(Pc)] spectrum,[6] Table S1 (Supporting Information), for comparison purposes. The observation of only one set of signals for the α and β protons for the two unsubstituted Pc rings in both complexes confirms that these two compounds adopt symmetrical molecular structure, that is, [(Pc)M{Pc(OC_8H_{17})$_8$}M(Pc)]. However, among all the heterodinuclear lanthanide triple-decker compounds, complete assignment of the spectra can be reached only for [(Pc)Lu{Pc(OC_8H_{17})$_8$}Yb(Pc)] (**15**) at this stage, even with the help of the 2D NMR spectra. As shown in the ^{1}H–^{1}H COSY spectrum (Figure 3), there are two sets of intercorrelated signals at $\delta = 11.23$ and 9.23 ppm and $\delta = 7.98$ and 7.90 ppm; these signals are attributed to the Pc rings that are connected to the Yb and Lu metal, respectively. The remaining aromatic singlet signal at $\delta = 10.96$ ppm is clearly due to the ring protons of Pc(OC_8H_{17})$_8$.

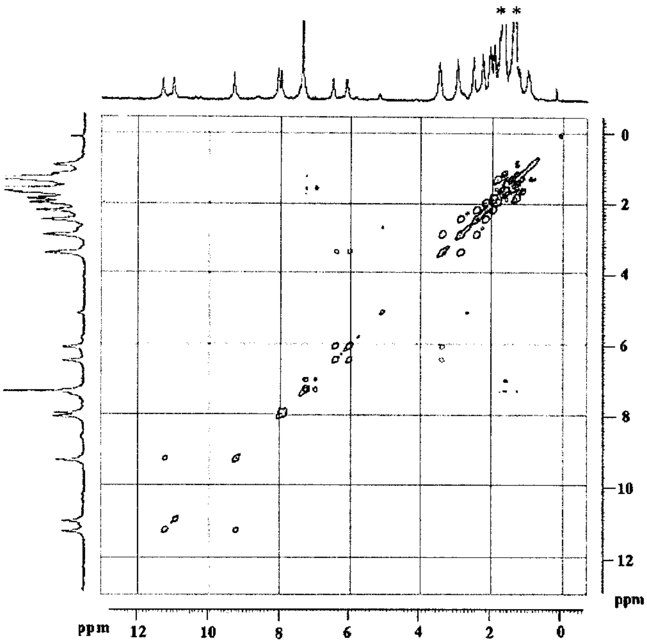

Figure 3. ^{1}H–^{1}H COSY spectrum of [(Pc)Lu{Pc(OC_8H_{17})$_8$}Yb(Pc)] (**15**) in $CDCl_3$; * indicates impurities.

The signals for the aliphatic protons can also be assigned unambiguously with the help of the ^{1}H–^{1}H COSY spectrum, Figure 3 and Table S1 (Supporting Information). The two multiplets at $\delta = 6.00$ and 6.41 ppm are due to the diastereotopic OCH_2 methylene protons. The multiplets from $\delta = 1.82$–3.36 can be ascribed to the $OCH_2CH_2CH_2CH_2CH_2CH_2$ methylene protons. The remaining signals for the $OCH_2CH_2CH_2CH_2CH_2CH_2CH_2$ methylene and $-CH_3$ methyl protons are overlapped by the solvent signals at $\delta = 1.64$ and 1.31 ppm, which are correlated each other as shown in the ^{1}H–^{1}H COSY spectrum.

Structure studies: Single crystals of [(Pc)M{Pc-(OC_8H_{17})$_8$}M(Pc)] (M = Er, Lu; **5**, **8**, respectively) and [(Pc)Lu{Pc(OC_8H_{17})$_8$}Er(Pc)] (**13**) suitable for X-ray diffraction analysis were obtained by diffusing hexane onto a solution of the compounds in toluene. These compounds crystallize in the triclinic system with a $P\bar{1}$ space group. Both the homo- and heterodinuclear lanthanide compounds have similar crystal structures (Table 5). It is worth noting that structurally characterized tris(phthalocyaninato) rare-earth-metal compounds remain very rare so far, and to our knowledge limited to [Lu_2{Pc(15C5)$_4$}$_3$] [H_2Pc(15C5)$_4$ = tetra-([15]crown-5)-substituted phthalocyanine][17] and [(Pc)M(Pc)M{Pc(α-OC_5H_{11})$_4$}] (M = Sm, Gd, Lu) reported very recently.[18] Nevertheless, the complex **13** represents the first tris(phthalocyaninato) complex that contains two different rare earth metals to be structurally characterized.

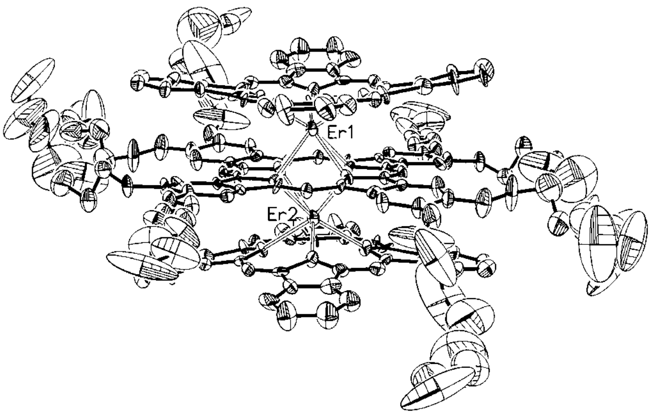

Figure 4. Side view of the molecular structure of [(Pc)Er{Pc(OC_8H_{17})$_8$}Er(Pc)] (**5**) with 30% probability thermal ellipsoids for all non-hydrogen atoms.

The molecular structure of [(Pc)Er{Pc(OC_8H_{17})$_8$}Er(Pc)] (**5**) is shown in Figure 4 (and in Figure S2 in the Supporting Information). As can be seen, each erbium ion is sandwiched between an outer phthalocyanine ligand Pc and the central Pc(OC_8H_{17})$_8$ ring. The two erbium ions in this compound are exactly identical, making the triple-decker molecule completely centrosymmetric. However, as shown in Table 3, the central Pc(OC_8H_{17})$_8$ ligand is not completely planar, arising from the interaction among the long octyloxy groups attached at the peripheral positions of the central phthalocyanine ligand Pc(OC_8H_{17})$_8$ between different triple-decker molecules in the crystal structure. The outer Pc ring adopts conformations that are domed towards the erbium cations ($\varphi = 9.1$). The outer Pc ring and the central Pc(OC_8H_{17})$_8$ ring connected by Er are rotated by an angle of 43.8° relative to their eclipsed conformation. The coordination polyhedron of Er is therefore almost a perfect square antiprism. The displacements of the erbium ion with respect to the four isoindole nitrogen atom mean planes are Er–N_4(Pc) = 1.217 Å and Er–N_4[Pc(OC_8H_{17})$_8$] = 1.712 Å, respectively. The average Er–N(Pc) bond length (2.332 Å) is significantly shorter than the average Er–N[Pc(OC_8H_{17})$_8$] distance (2.573 Å), as the central phthalocyanine ligand Pc(OC_8H_{17})$_8$ is shared by two erbium ions rather than one metal ion as is the case for the outer Pc ligand. This is also true for the molecular structure of homodilutetium compound **8** and heterodinuclear triple-decker **13**. As shown in Table 3, the ring-to-ring separation between the two neighboring ligands, as defined by the two N_4 mean planes, changes from 2.929 to 2.902 Å when the erbium in **5** is replaced by lutetium with a smaller ionic size in **8**. Whereas the separation between the two neighboring ligands in the heterodinuclear metal compound **13**, containing both Er and Lu, reasonably locates at 2.908 Å, exactly between those of the homodinuclear compounds **5** and **8**.

At the end of this section, it is must be pointed out that due to the very small difference in the atomic number between erbium and lutetium, discrimination of these two metals in the symmetrical triple-decker molecule of **13** was not possible with the present X-ray analysis technique.

Electrochemical properties: The electrochemical behavior of all the triple-decker complexes was investigated by cyclic voltammetry (CV) and differential pulse voltammetry (DPV) in CH_2Cl_2. These triple-decker compounds display four one-electron oxidations (labeled as Oxd_1–Oxd_4) and three one-electron reductions (Red_1–Red_3) within the electrochemical window of CH_2Cl_2 under the present conditions. The separation between the reduction and oxidation peak potentials for each process is 65–90 mV. All these processes are attributed to successive removal from, or addition of one electron to, the ligand-based orbitals, since the oxidation state of the central tervalent lanthanide ions in triple-decker complexes does not change. The half-wave redox potential values versus SCE are summarized in Table 4. Representative cyclic voltammogram and differential pulse voltammogram for [(Pc)Lu{Pc(OC_8H_{17})$_8$}Dy(Pc)] (**11**) are displayed in Figure 5.

Figure 6 shows the variation of the redox potentials of homodinuclear [(Pc)M{Pc(OC_8H_{17})$_8$}M(Pc)] (**1**–**8**) with the ionic radius of the lanthanide metal center. As can be seen in Figure 6 and Table 4, while the half-wave potentials

Table 3. Comparison of the structural data for **5**, **8**, and **13**.

	5	**13**	**8**
average M–N(Pc) bond length [Å]	2.332	2.283	2.30
average M–N[Pc(OC_8H_{17})$_8$] bond length [Å]	2.573	2.507	2.55
M–N_4(Pc) plane distance [Å]	1.217	1.213	1.202
M–N_4[Pc(OC_8H_{17})$_8$] plane distance [Å]	1.712	1.694	1.699
interplanar distance [Å]	2.929	2.908	2.902
dihedral angle between the two N_4 planes [°]	0.3	3.6	1.4
average dihedral angle ϕ for the Pc ring [°][a]	9.1	8.1	9.7
average dihedral angle ϕ for the Pc(OC_8H_{17})$_8$ ring [°][a]	4.65	7.05	4.05
average twist angle [°][b]	43.8	44.2	43.8

[a] The average dihedral angle of the individual isoindole rings with respect to the corresponding N_4 mean plane. [b] Defined as the rotation angle of the Pc ring away from the eclipsed conformation of the Pc and Pc(OC_8H_{17})$_8$ ring.

Table 4. Half-wave redox potentials of triple-deckers **1**–**15** in CH_2Cl_2 containing 0.1 M TBAP.

	Oxd_4	Oxd_3	Oxd_2	Oxd_1	Red_1	Red_2	Red_3	$\Delta E^{o}_{1/2}$[a]
1	+1.60	+1.21	+0.67	+0.32	−0.71	−1.06	−1.42	1.03
2	+1.60	+1.22	+0.66	+0.30	−0.70	−1.04	−1.38	1.00
3	+1.61	+1.22	+0.64	+0.29	−0.68	−1.03	−1.38	0.97
4	+1.60	+1.22	+0.64	+0.27	−0.68	−1.01	−1.35	0.95
5	+1.62	+1.23	+0.63	+0.26	−0.68	−1.03	−1.40	0.94
6	+1.60	+1.22	+0.61	+0.25	−0.70	−1.02	−1.41	0.95
7	+1.61	+1.23	+0.61	+0.23	−0.67	−1.01	−1.39	0.90
8	+1.62	+1.24	+0.60	+0.22	−0.67	−1.01	−1.39	0.89
9	+1.61	+1.23	+0.66	+0.29	−0.67	−1.00	−1.37	0.96
10	+1.63	+1.24	+0.66	+0.29	−0.68	−1.01	−1.37	0.97
11	+1.58	+1.23	+0.64	+0.27	−0.67	−1.01	−1.38	0.94
12	+1.61	+1.24	+0.63	+0.26	-0.66	-1.01	-1.38	0.92
13	+1.62	+1.24	+0.63	+0.25	−0.67	−1.02	−1.40	0.92
14	+1.58	+1.25	+0.62	+0.24	−0.66	−1.01	−1.38	0.90
15	+1.62	+1.23	+0.61	+0.23	−0.67	−1.01	−1.40	0.90

[a] $\Delta E^{o}_{1/2}$ is the potential difference between the first oxidation and first reduction processes, that is, the HOMO–LUMO gap of corresponding molecule.

Table 5. Crystallographic data for **5**, **8**, and **13**.

	5	**8**	**13**
formula	$C_{160}H_{176}N_{24}O_8Er_2$	$C_{160}H_{176}N_{24}O_8Lu_2$	$C_{160}H_{176}N_{24}O_8ErLu$
M_r	2897.77	2913.19	2905.48
crystal system	triclinic	triclinic	triclinic
space group	$P\bar{1}$	$P\bar{1}$	$P\bar{1}$
a [Å]	14.537(16)	14.513(12)	14.417(10)
b [Å]	15.396(19)	15.363(13)	15.258(10)
c [Å]	18.94(2)	18.828(16)	18.537(13)
α [°]	109.589(17)	109.214(13)	109.040(13)
β [°]	98.21(2)	98.417(13)	98.734(12)
γ [°]	109.727(18)	109.829(12)	109.716(11)
V [Å^3]	3600(7)	3568(5)	3468(4)
Z	1	1	1
ρ_{calcd} [Mg m^{-3}]	1.337	1.356	1.391
μ [mm^{-1}]	1.224	1.443	1.378
θ range [°]	1.51–24.00	1.96–24.00	1.53–24.00
reflections measured	13438	16248	15177
independent reflections	10314 ($R_{int}=0.1306$)	10791 ($R_{int}=0.0959$)	10167 ($R_{int}=0.2097$)
parameters	869	874	877
R_1 [$I>2\sigma(I)$]	0.0790	0.0709	0.0985
wR_2 [$I>2\sigma(I)$]	0.1093	0.0919	0.1755
goodness of fit	0.735	0.950	0.968

of the third and fourth oxidations of [(Pc)M{Pc(OC_8H_{17})$_8$}M(Pc)] remain virtually unchanged, the half-wave potentials of the first and second oxidations of these triple-deckers correlate linearly with the ionic size of the lanthanide metal center; these potentials are slightly shifted in the cathodic direction with decreasing radius of the lanthanide.

To understand the electrochemical data for these triple-decker complexes, the molecular orbital analysis method was employed. Accordingly, in these triple-decker molecules the close proximity of the three conjugated π-systems in a face-to-face configuration induces splitting of the doubly degenerate (e_g) LUMO and nondegenerate $4a_u$ HOMO molecular orbitals of the monophthalocyanines.[6,19] This results in three pairs of doubly degenerate unoccupied frontier molecular orbitals (the bonding LUMO, second nonbonding LUMO, and third antibonding LUMO) and three nondegenerate occupied frontier orbitals (the third bonding HOMO, second nonbonding HOMO and first antibonding HOMO) in the triple-deckers. The splitting between the first HOMO and second HOMO of triple-decker increases with decreasing lanthanide radius, due to the increase in the ring-to-ring interaction. Therefore, there is an increase in the energy of the antibonding HOMO in the same order, but no change in the energy of the nonbonding second HOMO. This is the reason why the half-wave potentials of the first and second oxidations (Oxd_1 and Oxd_2) dealing with the first antibonding HOMO are shifted slightly to the more negative direction along with the decrease of lanthanide radius and those for the third and fourth oxidations that are related to the second nonbonding HOMO are essentially unchanged. The half-wave potentials of all the three reductions for homodinuclear [(Pc)M{Pc(OC_8H_{17})$_8$}M(Pc)] (**1**–**8**) appear to reveal no systematic trends with ionic size, indicating that the degenerate LUMO does not change in energy along with the change in the lanthanide ionic size. As a result, the difference of the redox potentials of the first oxidation and first reduction for **1**–**8**, lying between 1.03 and 0.89 V, also decreases linearly with decreasing lanthanide radius, indicating enhanced π–π interactions in the triple-deckers with smaller lanthanides with respect to those connected by larger lanthanides. This result is supported by the optical properties of **1**–**8**. Electronic absorption studies have revealed that the lowest energy electronic absorption band at 692–722 nm in the electronic spectra of [(Pc)M{Pc(OC_8H_{17})$_8$}M(Pc)], which involves the electronic transition from the HOMO to the degenerate LUMO, is red-shifted along with the decrease of lanthanide ionic size.

The redox behaviors of the heterodinuclear compounds [(Pc)Lu{Pc(OC_8H_{17})$_8$}M(Pc)] (**9**–**15**) parallel those of their counterparts with two identical metals, see Table 4 and Figure 6. The redox potentials, especially those involving the

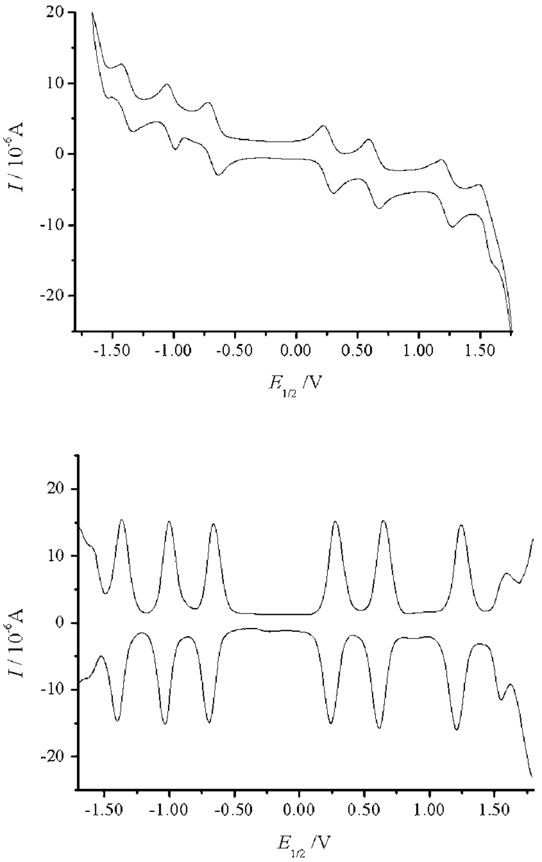

Figure 5. Cyclic voltammetry and differential pulse voltammetry of [(Pc)Lu{Pc(OC_8H_{17})$_8$}Dy(Pc)] (**11**) in CH_2Cl_2 containing 0.1 M [NBu_4][ClO_4] at scan rates of 20 (top) and 10 mVs^{-1} (bottom).

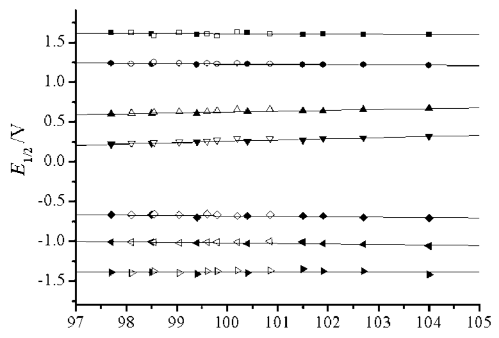

Figure 6. Plot of half-wave potentials of redox processes of [(Pc)M{Pc(OC_8H_{17})$_8$}M(Pc)] (**1**–**8**) (solid symbols) and [(Pc)Lu{Pc-(OC_8H_{17})$_8$}M(Pc)] (**9**–**15**) (open symbols) as a function of the ionic radius M^{III} and the mean ionic radius of Lu^{III} and M^{III}, respectively.

HOMO of [(Pc)Lu{Pc(OC_8H_{17})$_8$}M(Pc)], that is, the first and second oxidations, fit the linear correlation seen between the redox potentials and ionic radii for complexes with identical metals if the mean ionic radius of Lu and M is employed, Figure 6. This result clearly indicates the involvement of all three phthalocyanine rings in the frontier molecular orbitals of tris(phthalocyaninato) lanthanide compounds and the strong π–π interactions between the adjacent rings in the triple-decker molecules.

Conclusion

In summary, a series of homo- and heterodinuclear lanthanide tris(phthalocyaninato) complexes with symmetrical molecular structure [(Pc)M{Pc(OC_8H_{17})$_8$}M′(Pc)] (M = or ≠M′) have been prepared from the reaction of [(Pc)M{Pc(OC_8H_{17})$_8$}] and [(Pc)M′(acac)] facilitated by the eight electron-donating octyloxy groups at the peripheral positions of Pc(OC_8H_{17})$_8$ ligand. The compounds have been fully characterized with various spectroscopic and electrochemical methods. The molecular structures of these triple-deckers have also been determined by X-ray diffraction and NMR spectroscopy.

Experimental Section

General remarks: Anhydrous 1,2,4-trichlorobenzene (TCB) was purchased from Aldrich. Dichloromethane for voltammetric studies was freshly distilled from CaH_2 under nitrogen. Column chromatography was carried out on silica gel (Merck, Kieselgel 60, 70–230 mesh) with the indicated eluents. All other reagents and solvents were used as received. The compounds M(acac)$_3$·nH$_2$O,[20] [(Pc)M(acac)][21] and [(Pc)M{Pc-(OC_8H_{17})$_8$}] (M = Gd–Lu)[22] were prepared according to the published procedures.

Electronic absorption spectra were recorded on a Hitachi U-4100 spectrophotometer. MALDI-TOF mass spectra were taken on a Bruker BIFLEX III ultra-high-resolution Fourier transform ion cyclotron resonance (FT-ICR) mass spectrometer with α-cyano-4-hydroxycinnamic acid as matrix. Elemental analyses were performed by the Institute of Chemistry, Chinese Academy of Sciences. Electrochemical measurements were carried out with a BAS CV-50W voltammetric analyser. The cell was composed of inlets for a glassy carbon-disk working electrode of 2.0 mm in diameter and a silver-wire counter electrode. The reference electrode was Ag/Ag$^+$, which was connected to the solution by a Luggin capillary, whose tip was placed close to the working electrode. It was corrected for junction potentials by being referenced internally to the ferrocenium/ferrocene (Fe$^+$/Fe) couple [$E_{1/2}$ (Fe$^+$/Fe) = 501 mV vs SCE]. Typically, a solution of [Bu_4N][ClO_4] in CH_2Cl_2 (0.1 mol dm^{-3}) containing the sample (0.5 mmol dm^{-3}) was purged with nitrogen for 10 min, then the voltammograms were recorded at ambient temperature. The scan rates were 20 and 10 mV s^{-1} for CV and DPV, respectively.

General procedure for the preparation of [(Pc)M{Pc(OC_8H_{17})$_8$}M(Pc)] (M = Gd-Lu) (1–8) and [(Pc)Lu{Pc(OC_8H_{17})$_8$}M(Pc)] (M = Gd-Yb) (9–15): A mixture of [(Pc)M(acac)] (30 mg, 0.04 mmol) and [(Pc)M{Pc(OC_8H_{17})$_8$}] (0.025 mmol) in TCB (10 mL) was refluxed for about 10 h under a slow stream of nitrogen. The resulting blue solution was cooled to room temperature, and then the volatiles were removed under reduced pressure. The residue was subjected to chromatography with CH_2Cl_2 as eluent to give a dark-blue fraction containing the target heteroleptic tris(phthalocyaninato) compounds [(Pc)M{Pc(OC_8H_{17})$_8$}-M(Pc)] or [(Pc)Lu{Pc(OC_8H_{17})$_8$}M(Pc)] and a small amount of [(Pc)M(Pc)], which was repeatedly subjected to chromatography with toluene/hexane (3:1) to yield a deep blue fraction of the target triple-decker compounds. All compounds **1**–**15** were recrystallized from a mixture of toluene and hexane giving bluish violet crystals in the yields of 8–15%.

X-ray crystallographic analysis of 5, 8, and 13: Crystals suitable for X-ray diffraction analysis were grown by diffusing hexane onto a solution of the compounds in toluene. Crystal data and details of data collection and structure refinement are given in Table 5. Data were collected on a

Bruker SMART CCD diffractometer with $Mo_{K\alpha}$ radiation ($\lambda = 0.71073$ Å) at 293 K, using a ω scan mode with an increment of 0.3°. Preliminary unit cell parameters were obtained from 1290 frames. Final unit cell parameters were obtained by global refinements of reflections obtained from integration of all the frame data. The collected frames were integrated by using the preliminary cell orientation matrix. SMART software was used for collecting data, indexing reflections, and determination of lattice constants; SAINT-PLUS for integration of intensity of reflections and scaling;[23] SADABS for absorption correction;[24] and SHELXL for space group and structure determination, refinements, graphics, and structure reporting.[25] CCDC-248687–248689 contain the supplementary crystallographic data for this paper. These data can be obtained free of charge from The Cambridge Crystallographic Data Centre via www.ccdc.cam.ac.uk/data_request/cif.

Acknowledgement

Financial support from the Natural Science Foundation of China (Grant No. 20171028, 20325105), National Ministry of Science and Technology of China (Grant No. 2001CB6105), Ministry of Education of China, Shandong University for J.J., and The Chinese University of Hong Kong for D.K.P.N. is gratefully acknowledged.

---

[1] K. Kasuga, M. Ando, H. Morimoto, M. Isa, *Chem. Lett.* **1986**, 1095–1098.
[2] a) K. Takahashi, M. Itoh, Y. Tomita, K. Nojima, K. Kasuga, M. Isa, *Chem. Lett.* **1993**, 1915–1918; b) K. Takahashi, J. Shimoda, M. Itoh, Y. Fujita, H. Okawa, K. Nojima, *Chem. Lett.* **1998**, 173–174.
[3] a) F. Guyon, A. Pondaven, M. L'Her, *J. Chem. Soc. Chem. Commun.* **1994**, 1125–1126; b) F. Guyon, A. Pondaven, J.-M. Kerbaol, M. L'Her, *Inorg. Chem.* **1998**, *37*, 569–576.
[4] a) N. Ishikawa, Y. Kaizu, *Chem. Phys. Lett.* **1994**, *228*, 625–632; b) N. Ishikawa, Y. Kaizu, *Chem. Phys. Lett.* **1995**, *236*, 50–56; c) N. Ishikawa, Y. Kaizu, *Mol. Cryst. Liq. Cryst.* **1996**, *286*, 263–270; d) N. Ishikawa, T. Okubo, Y. Kaizu, *Inorg. Chem.* **1999**, *38*, 3173–3181.
[5] a) W. Liu, J. Jiang, D. P. Arnold, N. Pan, *Inorg. Chim. Acta* **2000**, *310*, 140–146; b) D. P. Arnold, J. Jiang, *J. Phys. Chem. A* **2001**, *105*, 7525–7533.
[6] P. Zhu, N. Pan, C. Ma, X. Sun, D. P. Arnold, J. Jiang, *Eur. J. Inorg. Chem.* **2004**, 518–523.
[7] N. Ishikawa, T. Iino, Y. Kaizu, *J. Am. Chem. Soc.* **2002**, *124*, 11440–11447.
[8] N. Ishikawa, T. Iino, Y. Kaizu, *J. Phys. Chem. A* **2002**, *106*, 9543–9550.
[9] N. Ishikawa, T. Iino, Y. Kaizu, *J. Phys. Chem. A* **2003**, *107*, 7879–7884.
[10] M. Elhabiri, R. Scopelliti, J.-C. Z. Bunzli, C. Piguet, *J. Am. Chem. Soc.* **1999**, *121*, 10747–10762.
[11] N. Martin, J.-C. Bünzli, V. McKee, C. Piguet, G. Hopfgartner, *Inorg. Chem.* **1998**, *37*, 577–589.
[12] G. Muller, J.-C. Bünzli, K. J. Schenk, G. Hopfgartner, *Inorg. Chem.* **2001**, *40*, 2642–2651.
[13] J. Lessmann, W. D. Horrocks, Jr., *Inorg. Chem.* **2000**, *39*, 3114–3124.
[14] N. Ouali, B. Bocquet, S. Rigault, P.-Y. Morgantini, J. Weber, C. Piguet, *Inorg. Chem.* **2002**, *41*, 1436–1445.
[15] a) J. Jiang, K. Kasuga, D. P. Arnold, in *Supramolecular Photosensitive and Electroactive Materials* (Ed.: H. S. Nalwa), Academic Press, New York, **2001**, chapter 2, pp. 113–210; b) D. K. P. Ng, J. Jiang, *Chem. Soc. Rev.* **1997**, *26*, 433–442.
[16] J. Jiang, W. Liu, D. P. Arnold, *J. Porphyrins Phthalocyanines* **2003**, *7*, 459–473.
[17] S. I. Troyannov, L. A. Lapkina, V. E. Larchenko, A. Yu. Tsivadze, *Dokl. Chem.* **1999**, *367*, 192–196.
[18] Y. Bian, L. Li, D. Wang, C.-F. Choi, D. Y. Y. Cheng, P. Zhu, R. Li, J. Dou, R. Wang, N. Pan, C. Ma, D. K. P. Ng, N. Kobayashi, J. Jiang, *Inorg. Chem*. accepted.
[19] X. Sun, R. Li, D. Wang, J. Dou, P. Zhu, F. Lu, C. Ma, D. K. P. Ng, J. Jiang, *Eur. J. Inorg. Chem.* **2004**, in press.
[20] J. G. Stites, C. N. McCarty, L. L. Quill, *J. Am. Chem. Soc.* **1948**, *70*, 3142–3143.
[21] M. Bai, X. Zhang, R. Li, P.-C. Lo, D. K. P. Ng, M. Bao, C. Ma, J. Jiang, unpublished results.
[22] a) J. Jiang, W. Liu, W.-F. Law, J. Lin, D. K. P. Ng, *Inorg. Chim. Acta* **1998**, *268*, 49–52; b) J. Jiang, J. Xie, M. T. M. Choi, Y. Yan, S. Sun, D. K. P. Ng, *J. Porphyrins Phthalocyanines* **1999**, *3*, 322–328.
[23] SMART and SAINT for Windows NT Software Reference Manuals, Version 5.0, Bruker Analytical X-Ray Systems, Madison, WI, **1997**.
[24] G. M. Sheldrick, SADABS, A Software for Empirical Absorption Correction, University of Göttingen, Germany, **1997**.
[25] SHELXL Reference Manual, Version 5.1, Bruker Analytical X-Ray Systems, Madison, WI, **1997**.

Received: August 26, 2004